

1. McMurdo Station (08/14/12 – 04/30/13)

Solar data of the SUV-100 spectroradiometer discussed in this quality control summary report encompass the period 08/14/12 – 04/30/13 and are part of Volume 22. A site visit took place between 1/28/13 and 1/31/13. The system performed normal and was stable before the site visit. Thereafter, the system's responsivity varied irregularly by about $\pm 6\%$. The effects of these variations were mostly removed by vicariously calibrating the system against the collocated GUV-511 multi-filter instrument. The uncertainty of the period 2/1/13 – 04/30/13 is increased by about 2%.

After performing the "season closing" calibrations at the beginning of the site visit, it was discovered that the third leg of the field calibrator (the leg without locking nuts) was not correctly seated in the base post because the leg was slightly bent. It is not clear whether also scans performed prior to the site visit were affected. Also the "season opening" scans (performed at the end of the site visit) had to be repeated because the leg was not seated correctly during the first series of scans.

The system's PSP radiometer S/N 12257F3 was replaced by PSP S/N 32760F3 during the site visit. Both instruments have been calibrated at NOAA before their installation on site. The calibration factor used for processing data of the period 8/14/12 - 1/28/13 using PSP S/N 12257F3 was $8.62 \times 10^{-6} \text{ V}/(\text{W m}^{-2})$. The calibration factor used for PSP S/N 12257F3 was $7.73 \times 10^{-6} \text{ V}/(\text{W m}^{-2})$.

1.1. Irradiance Calibration

The on-site irradiance standards used during the reporting period were the lamps M-543, 200W011, and 200W019. The three lamps have been in service at McMurdo for several years - see previous QC reports on their history. At the time of the site visit, the three lamps were compared against two traveling standards, lamps 200WN003 and 200W004. The results of this comparison led to the conclusion that the three on-site standards were in need for recalibration.

The three lamps were recalibrated against the traveling standard 200WN003 using absolute scans performed between 18:26z and 23:59z on 1/31/13. The standard 200WN003 had been calibrated at NOAA against lamps 200WN001 and 200WN002 on 3/21/13. Lamps 200WN001 and 200WN002 had in turn been calibrated at BSI in November 2012 against the NIST standard F-616 using a multi-filter transfer radiometer. NIST standard F-616 is traceable to the detector-based scale of irradiance established by NIST in 2000. At the time 200WN001 and 200WN002 were calibrated, they were also compared with the long-term traveling standard 200W017 of the NSF UV monitoring network. The irradiance scales of NIST standard F-616 and lamp 200W017 agreed to within 0.3%. It can therefore be assumed that the change from 200W017 to F-616 as the primary reference for calibrating on-site standards did not result in a significant step-change.

The SUV-100 system was somewhat unstable on the day of the calibration transfer (1/31/13). For example, a comparison of the two traveling standards 200WN003 and 200W004 using scans performed on 1/31/13 between 01:37z and 04:25z indicated a difference in their respective scales of +2%. A similar comparison using scans performed on the same day between 19:51z and 22:38z indicated a difference in their respective scales of -0.8%. The measurements performed at the later time were used for transferring the scale of irradiance of lamp 200WN003 to the on-site standards because they are considered the more reliable scans, in part because the field calibrator was seated correctly.

1.2. Instrument Stability

The temporal stability of the SUV-100 spectroradiometer was assessed by (1) analyzing measurements of the internal reference lamp, (2) analyzing absolute scans using the on-site standards, (3) comparing SUV-100 measurements with data of the collocated GUV-511 radiometer, and (4) comparing with results of a radiative transfer model. For method (3), SUV measurements are weighted with the spectral response functions of the GUV's channels

Figure 1 shows results from measurements of the internal lamp. Specifically, the readings of the instrument's TSI sensor are compared with measurements of the SUV-100's PMT at 300 and 400 nm. Between August 2012 and the start of the site visit, TSI readings decrease by about 3.5%, indicating that the internal lamp is getting dimmer. During the same period, PMT measurements vary by about $\pm 1.5\%$ with no apparent trend. After the site visit, TSI increase by about 2% while PMT measurements decrease by about the same amount. For a perfectly stable system, TSI and PMT measurements would track each other in response to a change in the lamp output. While this is not the case, the variations of both sensors are rather small, indicating that the internal parts of the system (monochromator, PMT) were stable to within $\pm 2\%$.

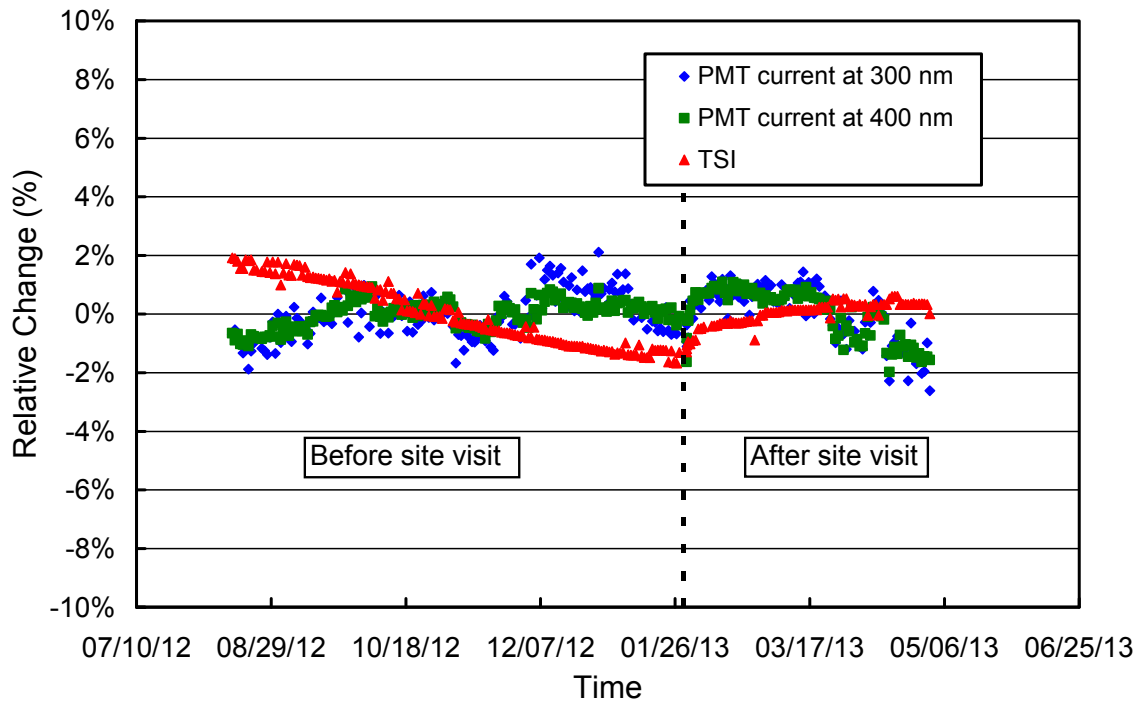


Figure 1. Measurements of the SUV-100's TSI sensor and PMT currents at 300 and 400 nm. The time of the site visit is indicated by a broken line. Data are shown as relative change, normalized to the average of measurements taken before and after the site visit.

Examination of scans of the site standards indicated that the system was quite stable between August 2012 and end of January 2013. After the site visit, data of the bi-weekly calibration events varied by about $\pm 7\%$ in the UV and $\pm 5\%$ in the visible, preventing the establishment of accurate calibrations based on absolute scans only. The high variability was confirmed by comparing measurements of the SUV-100 with data of the GUV-511. As an example, Figure 2 shows the ratio of GUV and SUV measurements at 340 nm.

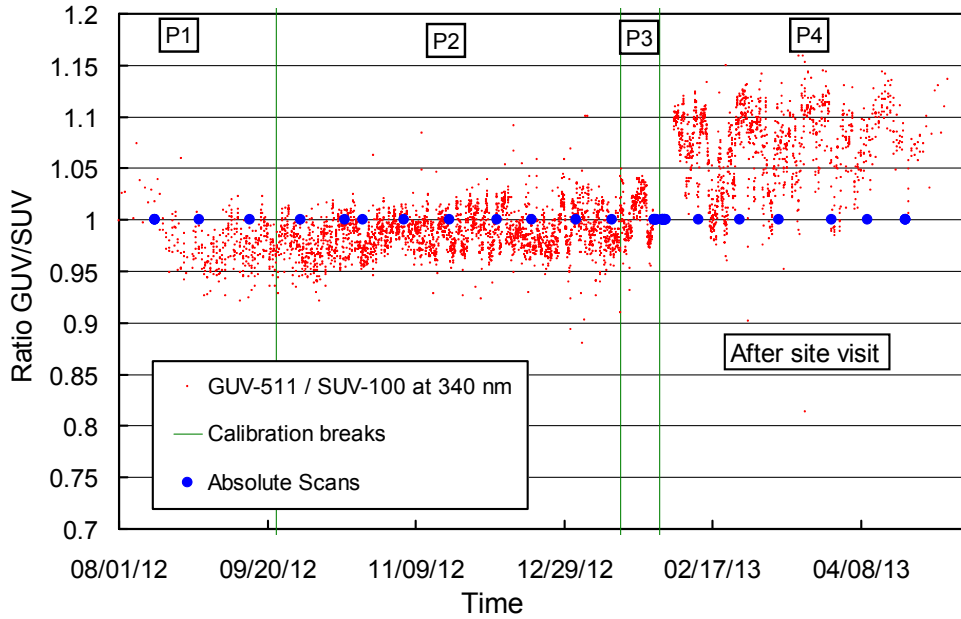


Figure 2. Ratio of GUV-511 measurements (340 nm channel) with preliminary SUV-100 measurements. Green vertical lines indicate times when the SUV-100 calibration was changed. Blue circles indicate times of the absolute scans. The calibration applied to solar data of Period P4 was calculated based on the average of absolute scans performed on 1/31/2013. A comparatively high variability is apparent in data of Period P4.

Before the site visit, normal calibration procedures were applied, resulting in three calibration periods, labeled P1 - P3 (Table 1). Figure 3 shows the ratios of irradiance assigned to the internal reference lamp during periods P2 and P3 relative to Period P1. Changes from period to period are smaller than 1%.

Table 1: Calibration periods for McMurdo Volume 22 data for solar data measured before the site visit.

Period name	Period range
P1	08/14/12 - 09/22/12
P2	09/23/12 - 01/16/13
P3	01/17/13 - 01/30/13

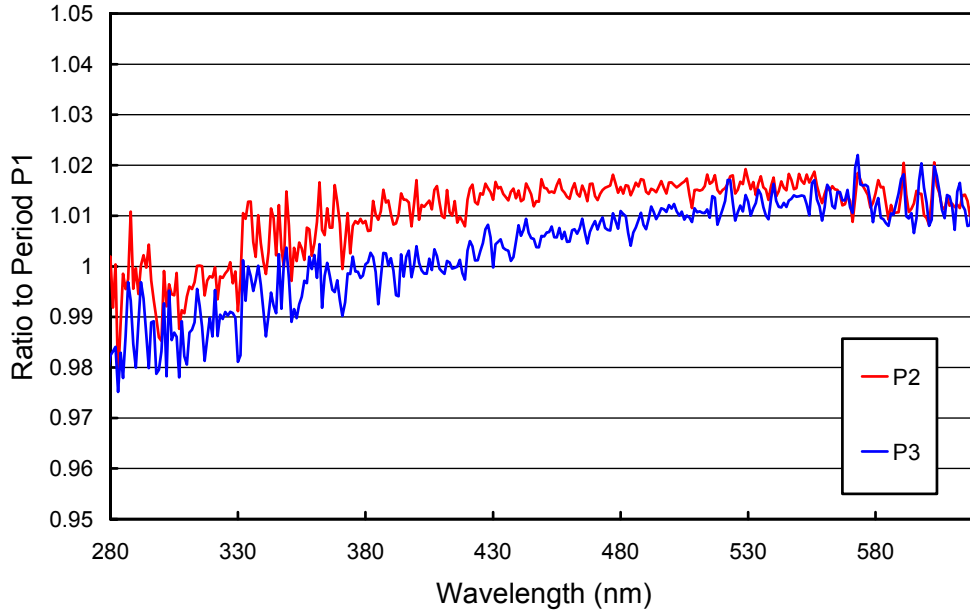


Figure 3. Ratios of irradiance assigned to the internal reference lamp during periods P2 and P3, relative to Period P1. Changes from period to period are smaller than 1%.

When solar data collected after the site visit (Period P4) is calibrated with a single calibration function, the GUV/SUV ratio at 340 nm varies by about $\pm 7\%$. The temporal spacing of absolute scans (blue circles in Figure 2) is too large to correct for this variability.

To correct for the instability in SUV-100 measurements the following procedure was applied:

- A calibration function was established using the absolute scan performed on 3/11/13. This day was selected because the ratio of GUV and SUV was fairly stable over a period of ± 2 days centered on 3/11/13. The calibration function is called $C_{70}(\lambda)$ where the subscript indicates the day-of-year (DOY). For 3/11/13, DOY = 70.
- For every day after the site visit, the average ratio of GUV and SUV measurements at 340 nm was determined and rounded to values of $R_{DOY}(340) = 0.92, 0.94, \dots 1.06$.
- The analysis of absolute scans indicated that the change in responsivity is somewhat wavelength dependent with smaller variations at longer wavelengths. The dependence can well be expressed with a linear function of wavelength. Hence, the variability of the SUV-100 at 600 nm, $R_{DOY}(600)$, was parameterized with: $R_{DOY}(600) = [(R(400) - 1) / 8 * 6] + 1$. For example, when $R_{DOY}(340) = 1.04$, $R_{DOY}(600) = 1.03$.
- For every day, a separate calibration function was established based on the following formula:

$$C_{DOY}(\lambda) = C_{70}(\lambda) \times \left[R_{DOY}(340) - \left(\frac{(R_{DOY}(340) - R_{DOY}(600)) \times (\lambda - 340)}{600 - 340} \right) \right]$$

and applied to solar data of Period P4.

- The comparison of GUV and SUV measurements using this calibration method was repeated and is shown in Figure 4. The step change between Periods P3 and P4 and the step-changes within Period P4, which were obvious in Figure 3, are largely absent in Figure 4. There is only a slightly larger variability in data of Period P4 compared to Period P2: the standard deviation of the GUV/SUV ratio is 2.0% for Period P2 and 2.2% for Period P4.

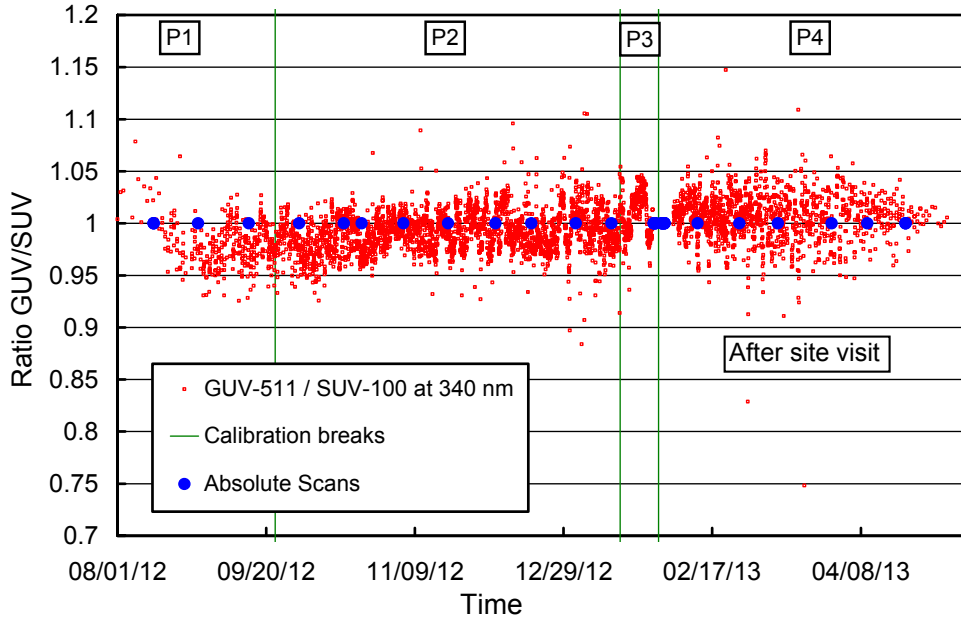


Figure 4. Ratio of GUV-511 measurements (340 nm channel) with final SUV-100 measurements. SUV measurements were weighted with the spectral response function of the GUV channel. Green vertical lines indicate times when the SUV-100 calibration was changed. Calibrations were changed on a daily basis in period P4 but this is not indicated in the graph.

Because of the uncertainty in the calibration of the traveling standard 200WN003 and the variability in the SUV-100 responsivity between February and April 2013 discussed above, additional measures were taken to ensure that solar data of the reporting period were calibrated correctly.

As part of Version 2 processing, clear-sky measurements are routinely compared against results of a radiative transfer model (e.g., Bernhard et al., 2004). The median of measurement/model ratios, calculated from all clear-sky data of a given volume, is typically constant to within $\pm 2\%$ from volume to volume. Figure 5 show these “median ratios” for Volumes 17 – 22. It can be seen that the ratio of Volume 22 data is consistent with those of the earlier Volumes, suggesting that solar data were calibrated correctly.

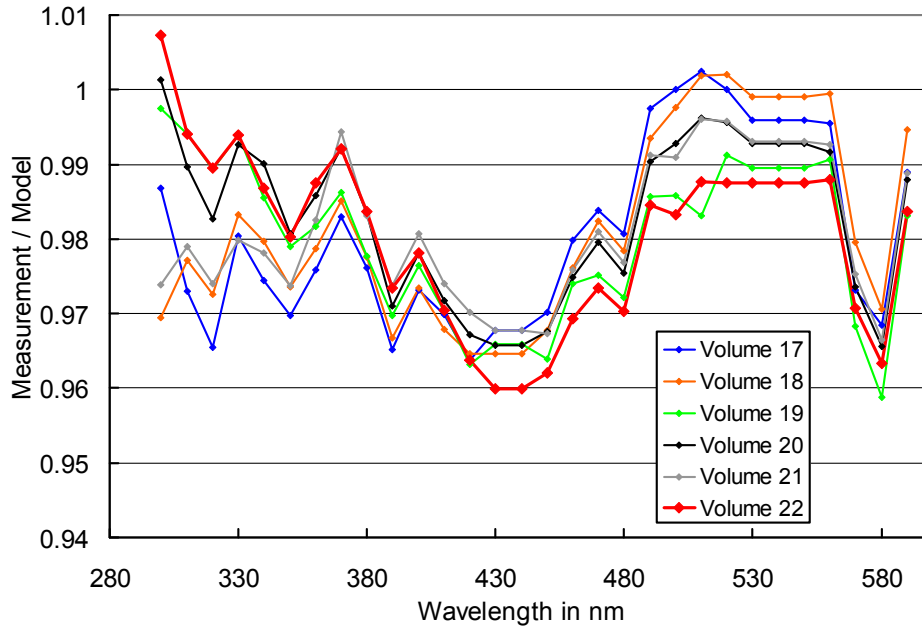


Figure 5. Median measurement/model ratios calculated from clear-sky solar measurements for data of Volumes 17 – 22. Ratios were averaged over 10 nm intervals (305-315, 315-325, ... 585-595 nm) before the median was calculated. There is a systematic, wavelength-dependent bias between measurement and model, however, this bias is generally to within $\pm 1\%$ for the six volumes, confirming that the irradiance scale used for processing of Volume 22 data is consistent with that used for earlier volumes.

As a last check to confirm that Volume 22 data were calibrated accurately, calibrated measurements of Volume 20, 21, and 22 for the same day of the year were directly compared. Such a comparison is only valid for periods that are free of clouds and have similar surface albedo. As an example for a period that meets these conditions, Figure 6 compares spectral irradiance measured on 9/17/11 (Volume 21 data) with similar data from 9/17/12 (Volume 22 data). The surface albedo was 0.83 on both days (surface albedo is a Version 2 data product) and measurements are consistent to within 1.5%. Figure 7 shows a similar example for 23-November, comparing Volume 20 data from 2010 and Volume 22 data from 2012. The albedo was 0.70 on 11/23/10 and 0.80 on 11/23/12. The datasets of 2010 and 2011 agree to within $\pm 3.0\%$. The slightly larger difference between the datasets indicated in Figure 7 (as compared to Figure 6) may be due to the difference in albedo, in particular at 340 nm.

The comparison with the model and the direct comparison of data from Volumes 20, 21, and 22 confirms that the calibration of Volume 22 solar data is consistent with historical data within the measurement uncertainty.

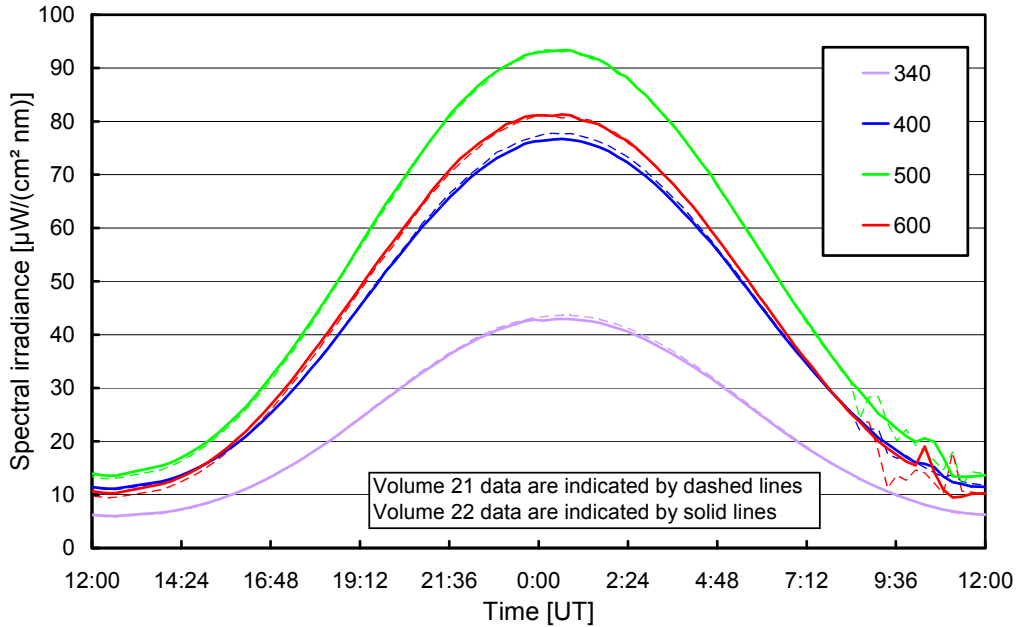


Figure 6. Spectral irradiance at 340, 400, 500 and 600 nm on 9/17/11 (Volume 21 data, dashed lines) and 9/17/12 (Volume 22 data, solid lines). The surface albedo was 0.83 on both days. The graph indicates that clear-sky measurements at the same time, one year apart, are consistent to within 1.5%.

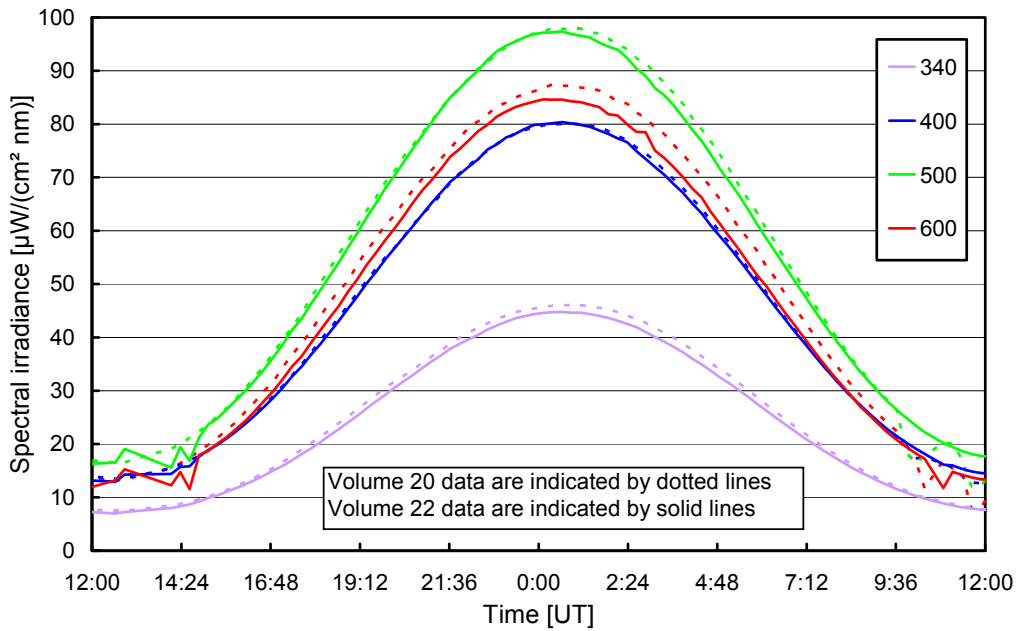


Figure 7. Spectral irradiance at 340, 400, 500 and 600 nm on 11/23/10 (Volume 20 data, dotted lines) and 11/23/12 (Volume 22 data, solid lines). The surface albedo was 0.70 on 11/23/10 and 0.80 on 11/23/12. The graph indicates that measurements at the same time, two years apart, are consistent to within 3%.

1.3. Wavelength Calibration

Wavelength stability of the system was monitored with the internal mercury lamp. Information from the daily wavelength scans was used to homogenize the data set by correcting day-to-day fluctuations in the wavelength offset. The wavelength-dependent bias of this homogenized dataset and the correct wavelength scale was determined with the Version 2 Fraunhofer-line correlation method (Bernhard et al., 2004). Figure 8 shows the correction functions calculated with this algorithm. Separate function was applied for solar data collected before (labeled Volume 22A) and after the site visit (Volume 22B).

Figure 9 indicates the wavelength accuracy of final Version 0 data for six wavelengths in the UV and visible that was established by running the Version 2 Fraunhofer-line correlation method a second time. Shifts are typically smaller than ± 0.05 nm. The wavelength correction was not modified when processing Version 2 data, which consequently have the same wavelength uncertainty of 0.02 nm (1σ) as Version 0 data.

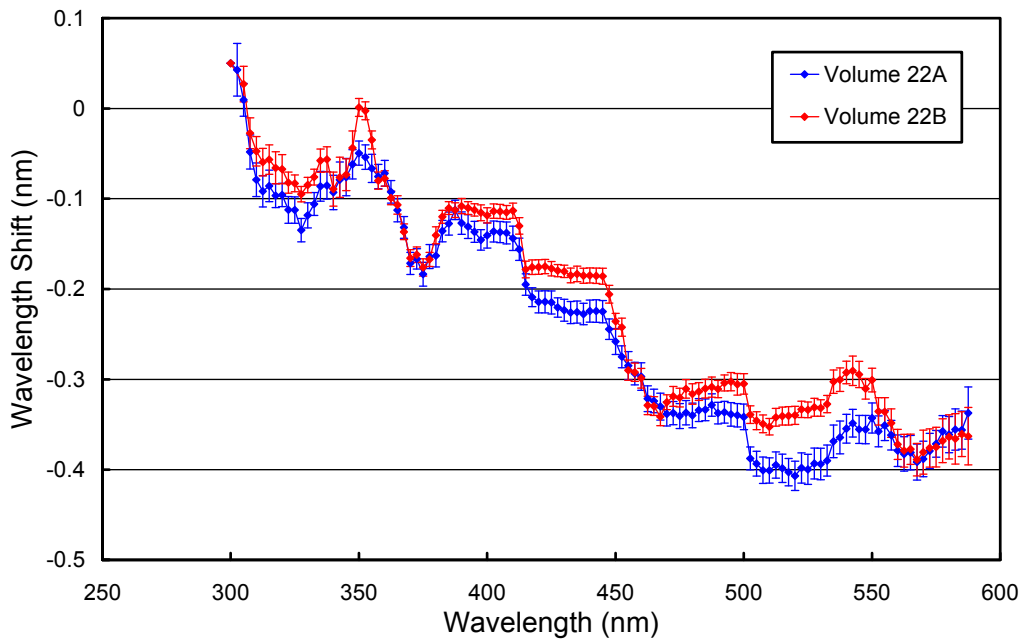


Figure 8. Monochromator non-linearity correction functions for the Volume 22 period. Error bars indicate the 1σ -variation. The function labeled “Volume 22A” was applied to solar data of the period 8/14/12 – 1/28/13 and the function labeled “Volume 22B” was applied solar data of the period 1/31/13 – 4/30/13.

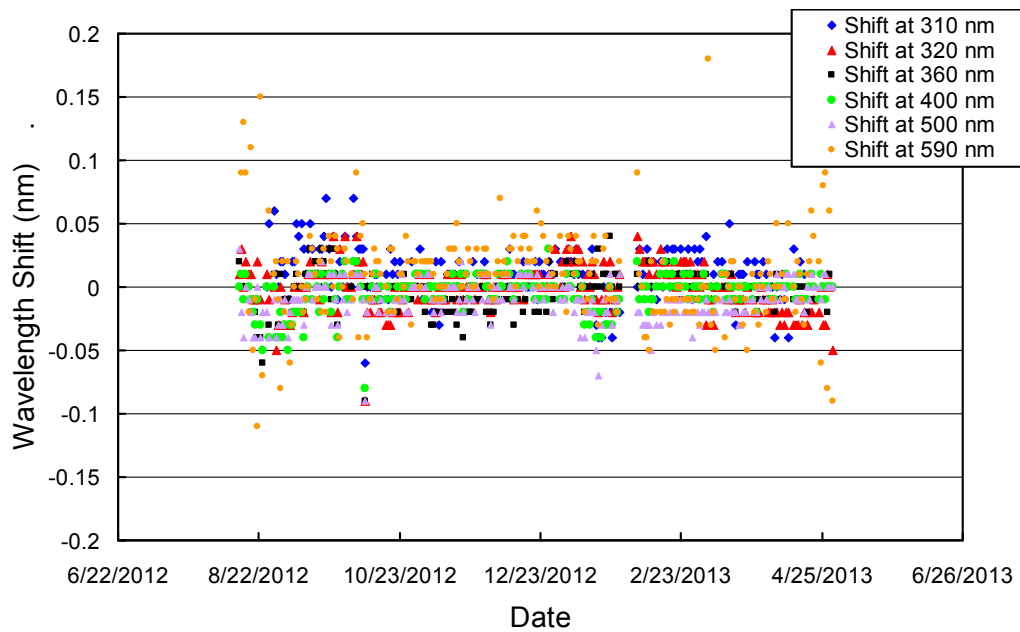


Figure 9. Check of the wavelength accuracy of final Version 0 data at six wavelengths by means of Fraunhofer-line correlation. The plot is based on daily measurements at noon.

References

Bernhard, G., C. R. Booth, and J. C. Ehamjian. (2004). Version 2 data of the National Science Foundation's Ultraviolet Radiation Monitoring Network: South Pole, *J. Geophys. Res.*, 109, D21207, doi:10.1029/2004JD004937.